Multi-response optimization of porous asphalt mixtures reinforced with aramid and polyolefin fibers employing the CRITIC-TOPSIS based on Taguchi methodology

C. J. Slebi-Acevedo [1], P. Pascual-Muñoz [1], P. Lastra-González [1] and D. Castro-Fresno [1,*]

[1] GITECO Research Group, Universidad de Cantabria, Avda. de Los Castros s/n, 39005 Santander, Spain.
* Correspondence: castrod@unican.es

Abstract: For the optimum design of a Porous Asphalt (PA) mixture, different requirements in terms of functionality and durability have to be fulfilled. In this research, the influence of different control factors such as binder type, fiber content, and binder content were statistically investigated in terms of multiple responses such as total air voids, interconnected air voids, particle loss in dry conditions, particle loss in wet conditions, and binder drainage. The experiments were conducted based on a Taguchi L18 orthogonal array. The best parametric combination per each response was analyzed through signal to noise ratio values. Multiple regression models were employed to predict the responses of the experiments. As more than one response is obtained, a multi-objective optimization was performed by employing Criteria Importance through Criteria Inter-Correlation (CRITIC) and Technique for Order Preference by Similarity to Ideal Solution (TOPSIS) methodologies. The weights for the selection of the functional and mechanical performance criteria were derived from the CRITIC approach, whereas the ranking of the different experiments was obtained through the TOPSIS technique. According to the CRITIC-TOPSIS based Taguchi methodology, the optimal multiple-response was obtained for a polymer-modified binder (PMB) with fiber and binder contents of 0.15% and 5.0%, respectively. In addition, good results were obtained when using a conventional 50/70 penetration grade binder with a 5.0% binder content and 0.05% fiber content.

Keywords: porous asphalt; fibers; Taguchi; Critic; Topsis.

1. Introduction

In the last 20 years, the use of porous asphalt (PA) mixtures in wearing courses has increased considerably around the world due to the multiple advantages that this type of hot mix asphalt (HMA) offers [1]. This mixture is characterized by the predominant use of high quality open-graded crushed coarse aggregates along with a small amount of fine aggregates in order to obtain a stone-on-stone contact and high interconnected air voids [2]. As a result, the granular skeleton formed is capable of resisting permanent deformation, whereas the connected voids allow the water to be evacuated from the surface of the pavement. Besides, when the water is removed, the splash and spray is minimized, as well as the aquaplaning effect [3]. Other advantages include the improvement of the pavement friction, especially in wet conditions, mist attenuation on rainy days, mitigation of the urban heat island effect, and enhancement of the surface reflectivity, especially in nighttime [4,5].

The porous structure of the PA mixture also contributes to mitigating the noise generated by the traffic loads [6]. In fact, porous asphalt pavements are currently the most widely used pavements worldwide when it comes to the reduction of the traffic noise [6–9]. As suggested by other researchers [6,10,11], the connected porous structure helps to dissipate the sound energy, whereas the surface pores and the macrotexture contribute to limit noise generation phenomena (i.e., air pumping or air sucking) in the tire-road contact.

45
46 Despite their multiple benefits, the high voids content makes the open graded mixtures prone to suffer
47 raveling [5], which can be defined as the loss of aggregate on the top of the surface during the service life
48 of pavement structure [12]. Moreover, due to their high porosity, a lower mortar content is present in PA
49 mixtures when compared to dense graded mixtures and hence, the adhesion between binder and
50 aggregates is worse. Similarly, as the mixture is highly exposed to the air and the wet conditions of the
51 environment, the binder film is susceptible to oxidation and consequently, the strength of the binder-
52 aggregate bonding is affected severely.
53
54 In order to improve the durability of the mix, several agencies around the world have employed different
55 admixtures. Open graded friction course (OGFC) mixtures, as they are called in the United States (US),
56 began to be used in the 1970s in response to a Federal Highway Administration program (FHWA) to
57 increase the frictional resistance on surface courses [13]. However, the applicability of OGFC mixtures was
58 relatively low until the 1980s, when the mix designs were improved by using polymer modified binder
59 (PMB) and fiber additives to stabilize the mix and prevent the drain down [4]. Similarly, China began to
60 apply porous asphalt courses in the 1980s. Nowadays, high-viscosity modified forms of asphalt binder are
61 used [5] for that purpose. Regarding Europe, Spain was one of the first countries that focused on the study
62 of PA mixtures [1,14]. In the 1980s, the University of Cantabria carried out a study based on developing a
63 design and control methodology [14]. As a result, the Cantabro test to evaluate the particle loss [15,16]
64 was developed and started to form part of the European standard methods (EN 12697-17). Also during
65 that period, the employment of porous asphalt mixtures as wearing course in The Netherlands became
66 very popular and widely used not only due to the road safety aspects, but also because of the potential
67 to mitigate the noise pollution from the traffic loads [17]. In this country, the modified binders are only
68 employed for special purposes [1]. Although the general tendency in Europe is towards the use of
69 modified binders as they possess higher flexibility and lead to thicker binder films with no binder drainage
70 [18], other researchers suggest that there is a lack of information proving the higher durability of the PA
71 mixtures using PMB [19]. In addition, although PMB brings ductility to the mixture due to the elastic
72 recovery properties and let the binder content to be increased [20], the use of additives such as fibers has
73 attracted much attention as it could prevent the draining of the binder while improving the mix durability
74 [21–23].
75
76 Several types of fibers have been used in hot asphalt mixtures: cellulose, polyester, carbon, basalt, glass,
77 polyacrylonitrile, nylon, or aramid, among others [24–30]. Asphalt concrete (AC) is the type of mixture
78 where the use of fibers as a reinforcement has been extensively used [26]. For example, Tapkin et al. [31]
79 reported 20% higher Marshall stability values when adding 0.3% polypropylene fibers by weight of
80 aggregates. Xu et al. [32] reported that polymer fibers such as polyester and polyacrylonitrile have greater
81 effects on the resistance to permanent deformation, fatigue life, and indirect tensile strength in
82 comparison to lignin and asbestos fibers. Similarly, the authors suggested an optimum fiber content of
83 0.35% by mass of mixture in order to achieve the best performance outputs with respect to rutting
84 resistance and indirect tensile strength. Takaikaew et al. [33] performed a detailed laboratory
85 experimental plan including Marshall stability, indirect tensile strength and stiffness modulus, resilient
86 modulus, dynamic creep, indirect tensile fatigue, and rutting resistance tests on asphalt concrete mixtures
87 with different types of binder (conventional, rubber modified asphalt and polymer modified asphalt) and
88 polyolefin/aramid fibers. According to the results, the addition of 0.05% of fibers by weight of mixtures
89 considerably improved the mechanical performance of the mixture, regardless of the asphalt binder type
90 used. Similarly, Kaloush et al. [34] reported that polypropylene/aramid fibers notably enhanced the
91 mixture's performance against rutting resistance, fatigue, and thermal cracking. Regarding the PA
92 mixtures, cellulose fibers have become the most common stabilizer additive [21,35–37]. Lopes et al. [21]
93 evaluated the performance of porous asphalt mixtures having cellulose fibers and polymer modified
94 binder. The authors concluded that cellulose fibers enables the increase of the binder content by
95 providing proper retention, thus resulting in greater aggregates coating and improved durability of the
96 mix. Similar results were obtained by Valeri et al. [36], who assessed the durability of a PA mixture

97   incorporating cellulose fibers but using a conventional 50/70 penetration grade bitumen instead of a
98   modified binder.
99
100   While good mechanical performance has been observed when using polyolefin/aramid (POA) fibers in
101   asphalt concrete mixes, the use of this fiber type has not been tested in PA mixtures. Additionally, many
102   studies have focused on the effects of fibers in only one category of bitumen, either a conventional binder
103   or a polymer-modified binder, but not both. Likewise, the use of fibers has only been valued as a stabilizer
104   additive and not as a reinforcement additive. Besides, the design of a porous asphalt mixture reinforced
105   with fibers requires optimum binder and fiber contents that guarantees an adequate resistance to
106   raveling and to the harmful action of the water, the absence of binder drainage, and a big enough air voids
107   content to enable the water to be removed from the surface and reduce the rolling noise.
108
109   In order to comply with the aforementioned, POA fibers are here presented as an alternative additive for
110   the stabilization of the mixtures and the improvement of their raveling resistance with no harm of their
111   optimal functionality. Furthermore, the novel CRITIC—TOPSIS based on Taguchi optimization technique
112   is proposed for the design of porous asphalt mixtures with the aim of finding out the most relevant input
113   parameters from the standpoint of their functionality and durability. In other words, the relationship
114   between type of binder, fiber content, and binder content are considered as the main control factors to
115   estimate the optimal solution for the mixture. As dependent variables or responses, total air voids,
116   interconnected air voids, raveling resistance in dry conditions, raveling resistance in wet conditions, and
117   binder drain down are considered.
118
119   The paper begins with an introduction section where the literature review of previous related research
120   works, scope and objectives of this study are referred. This section is followed by a detailed explanation
121   of the CRITIC—TOPSIS employed here based on the Taguchi novel technique. Materials and research
122   methods are thoroughly described in the third section, including material properties, sample preparation
123   and experimental testing plan. Results and discussion in section four describes main findings and includes
124   the statistical analysis performed and the different regression models aimed at predicting the response
125   values. The transformation of the multi-response into a single response through the CRITIC—TOPSIS
126   approach is also described. Finally, the main conclusions are drawn in the last section.

127   **2. Experimental Design**

128   *2.1. Taguchi Method*

129   The Taguchi method has been considered by other researchers as an efficient statistical method to
130   optimize the analysis of experimental variables and improve the accuracy of the responses [38,39].
131   Additionally, this method estimates the contribution of individual control factors that influence the quality
132   of a design process or optimum mix [40]. Although initially developed to improve the quality of
133   manufactured products, its use was extended to the civil engineering field [41–45].
134
135   In this study, the design of experiments was carried out according to the Taguchi L_{18} full factorial
136   orthogonal array ($2^1 \times 3^2$) in order to investigate the relationship between different binder and fiber
137   contents for different types of binders. Their effects on the durability and functionality of the PA mixture
138   were also analyzed.
139
140   The signal to noise ratio (SNR) is a measure that enables the determination of significant input parameters
141   by assessing the minimum variance [42]. In other words, higher values of SNR suggest more relevance of
142   the input parameters on the responses. In general SNR can be specified in three different scenarios
143   namely the *smaller-the-better*, the *larger-the-better*, and the *nominal-the-better*. In this research, the
144   smaller-the-better scenario is employed to minimize the loss of particles in dry and wet conditions as well
145   as the binder drainage, while the larger-the-better is employed to maximize the total air and

146 interconnected air voids. The equations used for calculating the *smaller-the-better* and the *larger-the-*
147 *better* scenarios are (1) and (2), respectively:

$$\frac{S}{N} = -10 \log_{10}\left(\frac{1}{n}\sum_{i=1}^{n} y_i^2\right) \tag{1}$$

$$\frac{S}{N} = -10 \log_{10}\left(\frac{1}{n}\sum_{i=1}^{n} \frac{1}{y_i^2}\right) \tag{2}$$

148 where y_i corresponds to the experimental result at the *i*th experiment and *n* refers to the total number
149 of experiments [42]. Binder type (50/70, PMB), Fiber content (*FC*) and binder content (*BC*) were selected
150 as control input parameters and their corresponding levels were determined as shown in Table 1. Thus,
151 18 sets of experiments with three replicates per design were carried out. Table 2 presents the L18 mixed
152 orthogonal array for conducting the design of experiments.

153

Table 1. Input parameters and their corresponding levels.

Input Parameter	Notation	Level 1	Level 2	Level 3
Binder type	BT	50/70	PMB	-
Fiber content (%)	FC	0.00	0.05	0.15
Binder content (%)	BC	4.5	5.0	5.5

154

Table 2. Full factorial design with Taguchi orthogonal array L18.

Design	Binder Type	Fiber Content	Binder Content
1	50/70	0.00	4.50
2	50/70	0.00	5.00
3	50/70	0.00	5.50
4	50/70	0.05	4.50
5	50/70	0.05	5.00
6	50/70	0.05	5.50
7	50/70	0.15	4.50
8	50/70	0.15	5.00
9	50/70	0.15	5.50
10	PMB45/80-65	0.00	4.50
11	PMB45/80-65	0.00	5.00
12	PMB45/80-65	0.00	5.50
13	PMB45/80-65	0.05	4.50
14	PMB45/80-65	0.05	5.00
15	PMB45/80-65	0.05	5.50
16	PMB45/80-65	0.15	4.50
17	PMB45/80-65	0.15	5.00
18	PMB45/80-65	0.15	5.50

155   *2.2. Technique for Order of Preference by Similarity to Ideal Solution (TOPSIS)*

156   The TOPSIS approach is considered one of the most popular mathematical models to determine the
157   optimal solution of a multi-criteria decision-making analysis (MCDM). In civil engineering, TOPSIS is
158   considered the second most popular multi-criteria technique right after the analytic hierarchy process
159   (AHP) [46]. Zhang et al. [47] evaluated public transport priority performance by applying TOPSIS. Jato et
160   al. [48] implemented an hybrid decision support model incorporating TOPSIS to rank different wearing
161   courses in highly trafficked European roads. On another study, Egle and Jurgita [49] ranked many
162   alternatives in order to improve the daylighting in vernacular buildings.

164   Unlike in previous investigations, in this research TOPSIS was adopted to transform the multi response
165   problem resulting from the design of experiments into a single response problem, thus giving the best set
166   of alternatives. Total air voids, interconnected air voids, particle loss in dry conditions, particle loss under
167   the influence of water, and binder drainage were considered to be the quality criteria required for TOPSIS
168   to set those reinforced porous asphalt alternatives.

170   The algorithm of TOPSIS is structured on the basis of the concept of distance of the alternatives proposed
171   to positive and negative ideal solutions [50]. In other words, a positive ideal solution (PIS) refers to an
172   alternative that maximizes the benefit responses and minimizes the cost responses, whereas a negative
173   ideal solution (NIS) is considered the least preferred solution as it minimizes the benefit responses and
174   maximizes the cost responses. Therefore, the best alternative would be the one closest to the positive
175   ideal solution and furthest from the negative ideal solution [51].

177   Following, the steps involved in the TOPSIS technique are presented.

179   **Step 1.** Build the decision-making matrix, with alternatives representing input parameters from the
180   manufacturing of asphalt mixes and criteria (or attributes) corresponding to the responses generated by
181   the experimental results. In line with this, the matrix can be expressed as follows:

$$P = \begin{pmatrix} p_{11} & p_{12} & \cdots & p_{1j} & \cdots & p_{1n} \\ p_{21} & p_{22} & \cdots & p_{2j} & \cdots & p_{2n} \\ \vdots & \vdots & \ddots & \cdots & \cdots & \vdots \\ p_{i1} & p_{i2} & \vdots & p_{ij} & \cdots & \vdots \\ \vdots & \vdots & \vdots & \vdots & \ddots & \vdots \\ p_{m1} & p_{m2} & \cdots & p_{mj} & \cdots & p_{mn} \end{pmatrix} \qquad (3)$$

182   where p_{ij} corresponds to the performance of the *i*th experimental alternative with respect to the *j*th
183   attribute.

185   **Step 2.** Normalize the decision matrix as follows

$$r_{ij} = \frac{p_{ij}}{\sqrt{\sum_{i=1}^{m} p_{ij}^2}}, \quad i = 1,2,3,\dots,m \quad j = 1,2,3,\dots,n \qquad (4)$$

186   where r_{ij} refers to the normalized rating of the attribute. In this step, various attribute dimensions are
187   transformed into non-dimensional attributes in order to make possible the comparisons across the
188   responses.

190   **Step 3.** Calculate the weighted normalized decision matrix as follows

$$[v_{ij}] = [w_j r_{ij}] \qquad (5)$$

191   where $[v_{ij}]$ corresponds to the weighted normalized matrix and w_j refers to the weightage of the *j*th
192   criterion. The following should be fulfilled

$$\sum_{j=1}^{n} w_j = 1. \qquad (6)$$

5

193 **Step 4.** Calculate the positive (PIS) and negative ideal solutions (NIS).

194

195   The positive ideal solution is determined as follows

$$V^+ = (v_1^+, v_2^+, v_3^+, \dots v_n^+) = \left\{ \left(max\ v_{ij} \big| j \in I \right), \left(min\ v_{ij} \big| j \in J \right) \right\} \qquad (7)$$

196   The negative ideal solution is determined as follows

$$V^- = (v_1^-, v_2^-, v_3^-, \dots v_n^-) = \left\{ \left(min\ v_{ij} \big| j \in I \right), \left(max\ v_{ij} \big| j \in J \right) \right\} \qquad (8)$$

197 where I is related with beneficial criteria and J with non-beneficial criteria; $i = 1,2, \dots, m$; and $j =$
198 $1,2, \dots, n$.

199

200 **Step 5.** Determine the distance of each alternative from positive and negative ideal solutions.

201

202   The distance to the positive ideal solution is as follows

$$S_i^+ = \sqrt{\sum_{j=1}^n \left(v_{ij} - v_j^+ \right)^2}, i = 1,2 \dots, m. \qquad (9)$$

203   The distance to the negative ideal solution is as follows

$$S_i^- = \sqrt{\sum_{j=1}^n \left(v_{ij} - v_j^- \right)^2}, i = 1,2 \dots, m. \qquad (10)$$

204 **Step 6.** Calculate the relative closeness from each alternative to the positive ideal solution

$$C_c^* = \frac{d_i^-}{d_i^- + d_i^+} \qquad (11)$$

205 where C_c^* is the relative closeness coefficient; $i = 1,2, \dots m$; $0 \le C_c^* \le 1$.

206

207 **Step 7.** Rank the different alternatives and select the option with C_c^* closest to 1.

208 *2.3. Criteria Importance through Inter-Criteria Correlation (CRITIC)*

209 When multiple responses are involved in a decision-making problem, prioritizing one criterion against the
210 others turns out to be a complex task due to the nature of subjectivity. To avoid that, the CRITIC
211 methodology developed by Diakoulaki et al. [52] arose as an innovative approach in the category of Multi-
212 Objective Decision Making (MODM) methods. Based on this methodology, weights of relative importance
213 can be determined in an objective manner as correlated to certain criteria [53]. This has been applied in
214 different areas of the engineering as a decision support system, including manufacturing processes, supply
215 chain, and risk management [54,55]. As for the combination of design of experiments and multi-criteria
216 decision-making analysis, no research has been carried out so far, with responses being commonly
217 assigned based on criteria with equal weightage [56]. Therefore, this research seeks to employ a novel
218 approach by means of using a technique that does not require human participation and helps to
219 automatize decision making, along with the TOPSIS method, which enable going from a multi-response
220 problem to an optimized single response. Following this, a brief description of the CRITIC technique is
221 presented based on reference [52].

222

223 **Step 1.** Define the finite set *A* of *n* alternatives with respect to *m* evaluation criteria as follows:

$$A = \left[a_{ij} \right]_{n*m} = \begin{bmatrix} a_{11} & a_{12} & \cdots & a_{1m} \\ a_{21} & a_{22} & \cdots & a_{2m} \\ \vdots & \vdots & \ddots & \vdots \\ a_{n1} & a_{n2} & \cdots & a_{nm} \end{bmatrix} (i = 1,2,\dots,n \text{ and } j = 1,2,\dots m) \qquad (12)$$

224 where a_{ij} represents the response value of the *i*th alternative on the *j*th criterion.

225

226

227

6

228   **Step 2.** Normalize the decision matrix using the following equation

$$\bar{a}_{ij} = \frac{a_{ij} - a_j^{worst}}{a_j^{best} - a_j^{worst}} \tag{13}$$

229   where $\bar{a}_{ij}$ is the normalized performance value of the ith alternative for the jth criterion, a_j^{best}
230   corresponds to the best performance value for jth criterion, and a_j^{worst} is the worst performance value
231   for jth criterion.
232
233   **Step 3.** Calculate the standard deviation σ of each vector a_j, which quantifies the contrast intensity of the
234   corresponding criterion.
235
236   **Step 4.** Build the symmetric $m * m$ matrix with the generic element r_{jk}, which corresponds to the linear
237   correlation coefficient between vectors a_j and a_k.
238
239   **Step 5.** Determine with the following formula the measure of the conflict created by criterion j with
240   respect to the decision situation defined by the rest of the criteria

$$\sum_{k=1}^{m} 1 - r_{jk}. \tag{14}$$

241   **Step 6.** Calculate C_j, which represents the quantity of information contained in jth criterion.

$$C_j = \sigma * \sum_{k=1}^{m} 1 - r_{jk} \tag{15}$$

242   **Step 7.** Determine the objective weights of the jth criterion.

$$W_j = \frac{C_j}{\sum_{k=1}^{m} C_j} \tag{16}$$

243   **3. Materials and Methods**

244   *3.1. Materials*

245   In this study, ophite and limestone were used as coarse and fine aggregates, respectively, for the
246   manufacturing of the PA mixtures. Limestone was also employed as filler material. The gradation curve
247   corresponds to a PA mixture with nominal maximum aggregate of 16 mm commonly known as PA16 by
248   Spanish specifications [57]. The physical properties and gradation of aggregates can be seen in Table 3
249   and Figure 1, respectively. As for the bituminous binder, in this research a conventional 50/70 penetration
250   grade bitumen (50/70) and a polymer-modified binder (PMB 45/80-65) were used. The main properties
251   of the binders are shown in Table 4.
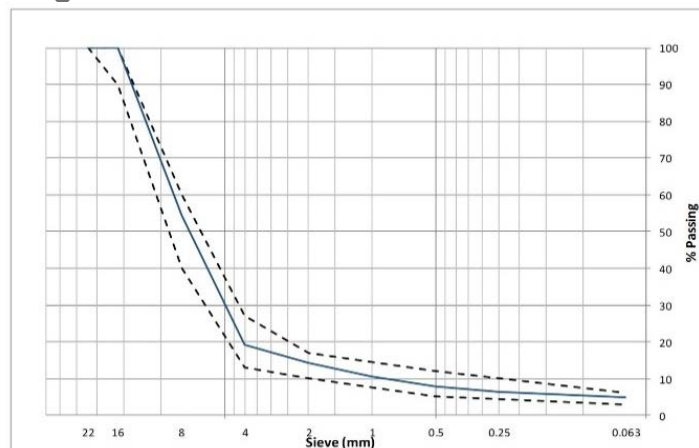
252

253   **Figure 1.** Gradation curve of the PA16 mixture.

254   Regarding the fibers, a blend of polyolefin and aramid synthetic fibers (POA) was used for both improving
255   the durability of the PA mixture and as a stabilizing additive. The density of the blend according to the
256   standard method UNE-EN 1097-6 is 0.947 g/cm^3. The main physical properties of the POA fibers and a
257   picture of them can be seen in Table 5 and Figure 2, respectively.

258

Table 3. Physical properties of coarse (ophite) and fine (limestone) aggregates.

Characteristic	Value	Standard	Specification
Coarse Aggregate			
Specific Weight (g/cm^3)	2.794	EN 1097-6	-
Water absorption (%)	0.60	EN 1097-6	<1%
L.A abrasion (%)	15	EN 1097-2	≤15%
Slab Index (%)	<1%	EN 933-3	≤20%
Polishing Value	60	EN 1097-8	≥56
Fine Aggregate			
Specific Weight (g/cm^3)	2.724	EN 1097-6	-
Sand Equivalent	78	EN 933-8	>55

259

Table 4. Main properties of the binders used.

Binder	Test	Standard Method	Value
50/70	Penetration at 25 °C (mm/10)	EN 1426	57.00
	Specific Gravity	EN 15326	1.04
	Softening point (°C)	EN 1427	51.60
	Fraass brittle point (°C)	EN 12593	−13.00
PMB 45/80-65	Penetration at 25 °C (mm/10)	EN 1426	49.50
	Specific Gravity	EN 15326	1.03
	Softening point (°C)	EN 1427	72.30
	Fraass fragility point (°C)	EN 12593	−15.00
	Ductility force at 5 °C (J/cm^2)	EN 13589	3.11
	Elastic recovery at 25 °C (%)	EN 13398	90.00

260

Table 5. Characteristics of POA fibers.

Fiber	Aramid	Polyolefin
Form	Monofilament	Serrated
Color	Yellow	Yellow
Density (g/cm^3)	1.44	0.91
Length (mm)	19	19
Tensile Strength (MPa)	2758	483
Decomposition temperature (°C)	>450	157
Acid/Alkali Resistance	Inert	Inert

8

262   **Figure 2.** Blend of polyolefin and aramid (POA) fibers.

263   *3.2. Manufacturing of the Porous Asphalt Sample*

264   For the manufacturing of the PA samples using conventional 50/70 penetration grade bitumen, coarse
265   and fine aggregates and the filler were first heated for six hours in an oven at 170 °C and then thoroughly
266   mixed with the fibers. Afterwards, the binder at 150 °C was placed into the mixture and continuously
267   blended until the combination fiber-aggregate was well coated. When the polymer modified binder was
268   used, the aggregates and binder temperatures increased from 170 °C to 185 °C and from 150 °C to 165
269   °C, respectively. Finally, all the test samples were compacted by 50 blows per side according to the EN
270   12697-30.

271   *3.3. Laboratory Testing Plan*

272   In order to optimize the functionality and durability of the PA mixture, total air voids, interconnected air
273   voids, binder drainage, and raveling resistance in dry and wet conditions have been considered as porous
274   asphalt quality criteria. Based on the volumetric properties test [58,59], total air voids (T_{AV}) and
275   interconnected air voids (I_{AV}) were calculated following the Equations (17) and (18), respectively:

$$T_{AV}(\%) = \left(1 - \frac{m}{V * G_{mm}}\right) * 100\% \tag{17}$$

$$I_{AV}(\%) = \frac{V - \frac{m - m_w}{\rho_w}}{V} * 100\% \tag{18}$$

276   where *m* corresponds to the mass of the specimen in the air; *V* refers to the total volume of the specimen,
277   which is calculated geometrically; G_{mm} is the theoretical maximum specific gravity of the mixture; and
278   m_w is the saturated specimen mass in water.
279
280   To assess the durability of the PA mixture in terms of its raveling resistance, the Cantabro loss particle test
281   (EN 12697-17) was carried out. According to this test, the particle loss refers to loss mass of a PA specimen
282   after applying 300 revolutions in the Los Angeles abrasion machine. The particle loss (*PL*) is calculated as
283   follows:

$$PL(\%) = \frac{w_1 - w_2}{w_2} * 100\% \tag{19}$$

284   where w_1 is the initial weight of the specimen and w_2 refers to the final weight of the specimen.
285
286   Additionally, the Cantabro test in wet conditions was performed following the Spanish standard method
287   NLT 362/92. Before the test, specimens were conditioned by submerging them in water at 60 °C for 24 h
288   and then exposed to air at 25 °C for another 24 h.

289

290   To assess the stability of the mixture, the mesh basket binder drain down test according to the EN 12697-
291   18 standard was used. The test consist of quantifying the material lost by drainage after 3h at the test
292   temperature [60]. The binder drainage (*BD*) in percentage is determined as follows.

$$BD\ (\%) = \frac{m_2 - m_1}{1100 + B} * 100 \tag{20}$$

293   where m_1 is the initial mass of the tray and foil, m_2 refers to the mass of the tray and foil including the
294   drained material, and B corresponds to the initial mass of the binder in the mixture.
295
296   The experimental part was developed in the roads laboratory of the University of Cantabria. The
297   structured framework of the multi-objective optimization can be observed in Figure 3.
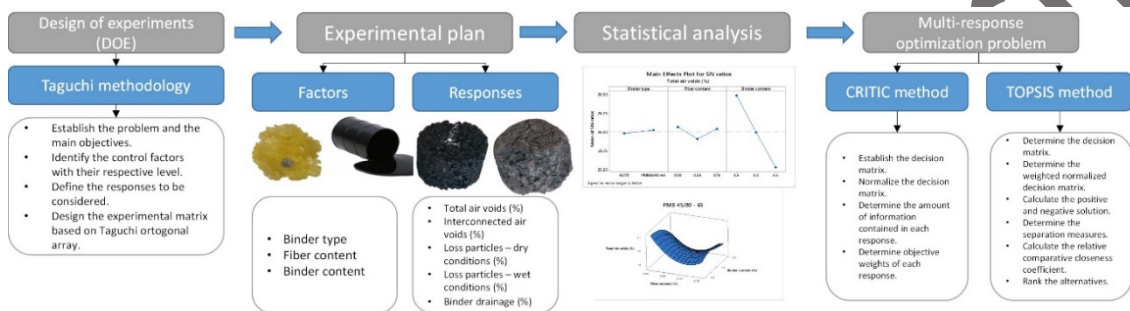
298
299   **Figure 3.** Structured framework proposed for the multi-objective optimization.

4. Results and Discussion

301   *4.1. Analysis of Signal to Noise Ratios (SNR) and Means on Different Responses*

302   The different responses obtained by way of the Taguchi L18 orthogonal array can be observed in Table 6.
303   Total and interconnected air voids are considered an important parameters to assess the functionality of
304   the PA mixture in terms of permeability, noise properties and macrotexture [61]. As for the results, mean
305   values of T_{AV} and I_{AV} ranged from 17.50% to 23.20% and 11.20% to 17.26%, respectively (Table 6).
306   Similarly, a direct relation exists between both responses, with a Pearson correlation coefficient of 89%.
307   Following the Taguchi methodology, T_{AV} and I_{AV} were converted into signal-to noise ratio (SNR). The
308   highest values of total and interconnected air voids are very important for improving the functional
309   performance of the mixture. Therefore, the *larger-the-better* equation was employed for calculating the
310   SNR. Figures 4 and 5 show the main effect of the SNR and the means for the total and interconnected air
311   voids, respectively.
312
313   A SNR analysis of the effect of the input factors, i.e., binder type (BT), fiber content (*FC*) and binder content
314   (*BC*), on the total and interconnected air voids was carried out (Figures 4 and 5). SNR makes it possible to
315   show the optimal levels of the different input factors for the optimal responses (T_{AV} and I_{AV}). As an
316   example, the levels and SNR for the factors giving the best T_{AV} response are: level 2 and SNR = 26.03 for
317   BT factor; level 1 and SNR = 26.07 for *FC* factor; and level 1 and SNR = 26.49 for *BC* factor. Therefore, the
318   optimum T_{AV} can be obtained by using a polymer modified binder, with the lowest binder content and no
319   fibers. Despite that, it is worth mentioning that the binder content is the input factor that most influences
320   the change in the air voids value in comparison to the binder type or fiber content, as can be observed in
321   Figure 4b and Figure 5b. On the other hand, the type of binder does not have a notable influence on the
322   T_{AV} response.

(a) (b)
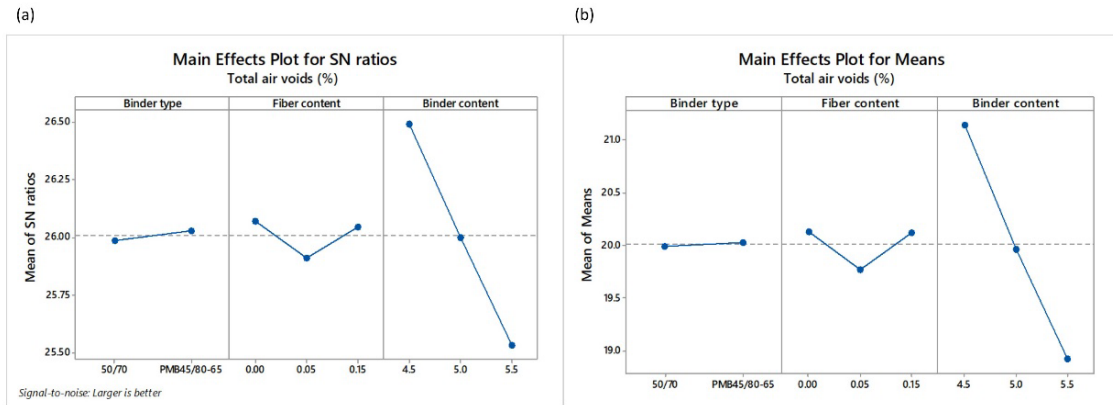
Figure 4. Main effects plots of (**a**) SNR and (**b**) means of the total air voids T_{AV}.

(a) (b)
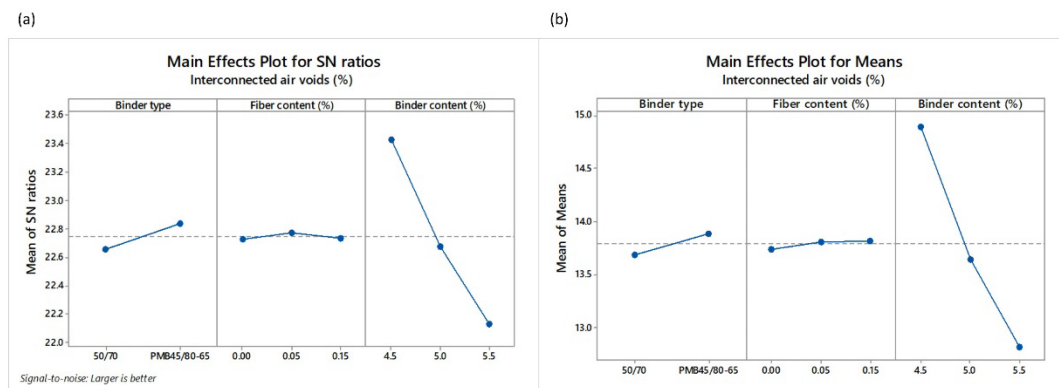
Figure 5. Main effects plots of (**a**) SNR and (**b**) means of the interconnected air voids I_(AV).

**Table 6.** L18 Taguchi orthogonal array response variables.

Design	Total Air Voids (T_{AV})		Interconnected Air Voids (I_{AV})		Particle Loss-Dry Condition (PL_{DRY})		Particle Loss-Wet Condition (PL_{WET})		Binder Drainage (BD)
	mean	SD	mean	SD	mean	SD	mean	SD	
1	21.39	0.75	14.59	1.32	14.96	1.99	19.12	5.51	0.01
2	18.85	0.14	12.45	0.70	6.76	2.65	15.32	3.20	0.40
3	18.68	1.12	11.94	1.48	9.37	0.75	8.28	2.03	2.25
4	21.36	0.35	15.59	1.01	12.52	1.99	39.85	10.23	0.01
5	19.67	0.40	13.57	0.61	7.90	4.27	15.71	1.89	0.03
6	18.85	0.14	12.45	0.70	4.90	1.68	10.70	1.40	0.59
7	23.22	0.22	17.26	0.38	19.71	2.01	35.95	5.05	0.02
8	20.38	0.88	14.14	1.06	15.66	1.86	22.74	3.15	0.01
9	17.49	1.30	11.22	0.99	7.01	1.39	9.08	2.15	0.16
10	20.59	1.89	14.36	2.22	10.57	4.80	10.81	3.54	0.00
11	21.12	0.40	15.16	0.80	5.16	2.77	7.19	1.68	0.28
12	20.18	2.18	13.93	2.91	4.73	0.78	7.49	1.72	0.97
13	20.81	2.14	14.47	2.66	5.94	2.20	7.80	3.52	0.00
14	19.54	1.88	12.39	2.80	8.12	5.19	5.62	0.26	0.04
15	18.42	2.51	14.39	3.43	2.52	0.96	8.25	2.47	0.12
16	19.50	1.14	13.12	0.91	8.47	3.70	7.73	0.45	0.04
17	20.22	0.17	14.15	0.11	4.77	1.02	5.26	0.76	0.05
18	19.91	1.03	13.03	0.97	3.30	0.34	3.48	0.62	0.21

328 Concerning the evaluation of the mechanical performance, raveling resistance was evaluated on Marshall
329 Samples in dry and wet conditions.
330
331 Mean values of the three replicas per design and test along with their corresponding standard deviations
332 can be observed in Table 6. It is also interesting to notice that a direct correlation between the loss
333 particles in dry and wet conditions exists, with a Pearson correlation coefficient of 79%. It means that the
334 lower the values of particle loss in dry conditions (PL_{DRY}) are, the lower the values of particle loss in wet
335 conditions (PL_{WET}) are, too. Figures 6 and 7 depicts the main effects of SNR as well as the means for the
336 loss of particles in dry and wet conditions, respectively. Contrary to the calculation of air voids, the
337 *smaller-the-better* quality characteristics were used to calculate the SNR. The highest value of SNR
338 determines the best level for each control factor. For example, the levels and SNR for the input factors
339 giving the optimal value of PL_{DRY} are: level 2 and SNR = −14.72 for BT factor; level 2 and SNR = −15.90 for
340 *FC* factor; and level 3 and SNR = −13.70 for *BC* factor. This means that the optimum value of PL_{DRY} is
341 obtained when polymer modified binder is used along with 0.05% POA fibers and 5.5% binder content. As
342 for the PL_{WET} value, the highest impact according to SNR values comes from the binder type and the
343 binder content. In fact, the contribution of fibers in terms of raveling resistance under the water action is
344 less appreciable when a polymer-modified binder is used, as can be observed in the main effect plots for
345 the means (Figure 7b).
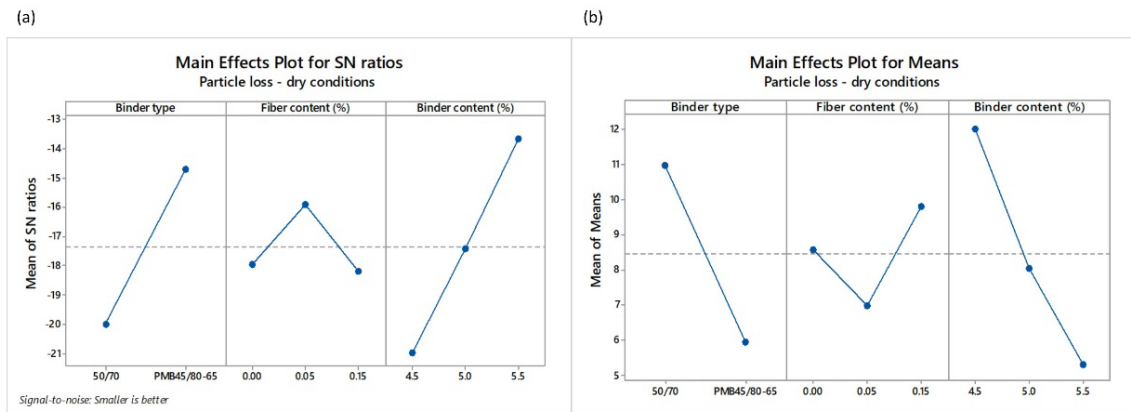
346
347 **Figure 6.** Main effects plots of (**a**) SNR and (**b**) means of the particle loss in dry conditions PL_{DRY}.
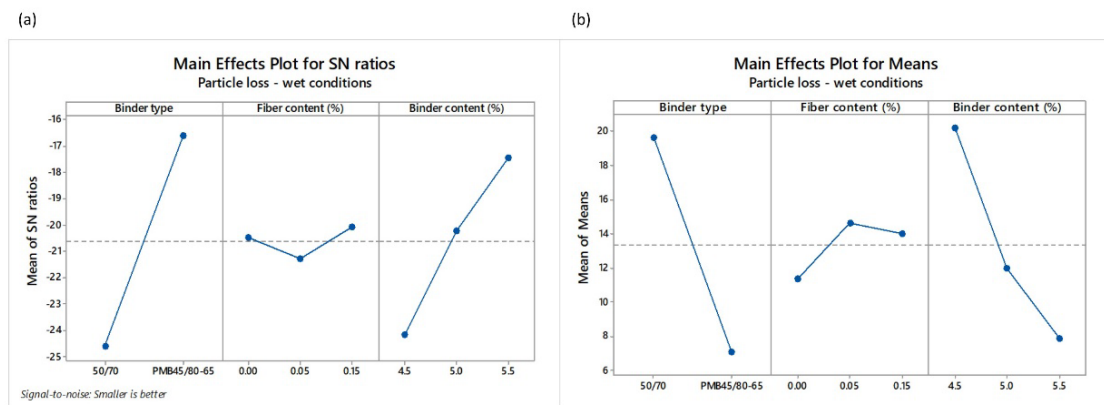
348
349 **Figure 7.** Main effects plots of (**a**) SNR and (**b**) means of the particle loss in wet conditions PL_{WET}.

350 The non-compacted PA mixtures corresponding to all the designs were subjected to evaluation of their drain
351 down characteristics through the mesh basket drain down test as per the EN 12697-18 standard. Binder
352 drainage (*BD*) results are shown in Table 6. As well as to evaluate the raveling resistance, *smaller-the-better*
353 equation was chosen to calculate the SNR values, as can be seen in Figure 8. According to the results, the

354 levels and SNR values for the factors giving the less binder drainage were: level 1 and SNR = 22.87 for the
355 BT factor; level 3 and SNR = 26.24 for the *FC* factor; and level 1 and SNR = 35.49 for the *BC* factor. In other
356 words, the lowest binder drainage can be obtained when a conventional 50/70 penetration grade binder
357 is used along with 0.15% POA fibers and 4.5% binder content. The reduced value of *BC* (Figure 8b) might
358 suggest that fibers can absorb the free binder in the mix.
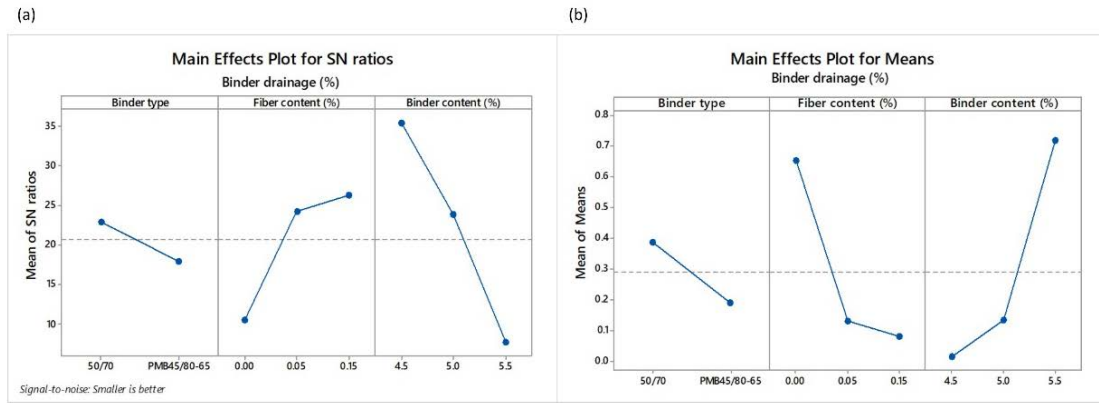
359

360 **Figure 8.** Main effects plots of (**a**) SNR and (**b**) means of the binder drainage (*BD*).

361 *4.2. Statistical Analysis of Response Results*

362 The changes in the different responses obtained as a result of the experimental research are shown in
363 Figure 9. The interaction effect between binder content and fiber content is plotted as depending of the
364 binder type per each response value (T_{AV}, I_{AV}, PL_{DRY}, PL_{WET}, BD). For practical reasons, which are based
365 on the response variable data obtained from tests with mixtures with 50/70 penetration grade binder, an
366 analysis of variance was performed. A 5% significance level and a 95% confidence level were considered
367 for the calculation of the factors affecting the different output parameters (Table 7). The significance of
368 the input parameters in the analysis of variance was identified by comparing the *F*-values of each input
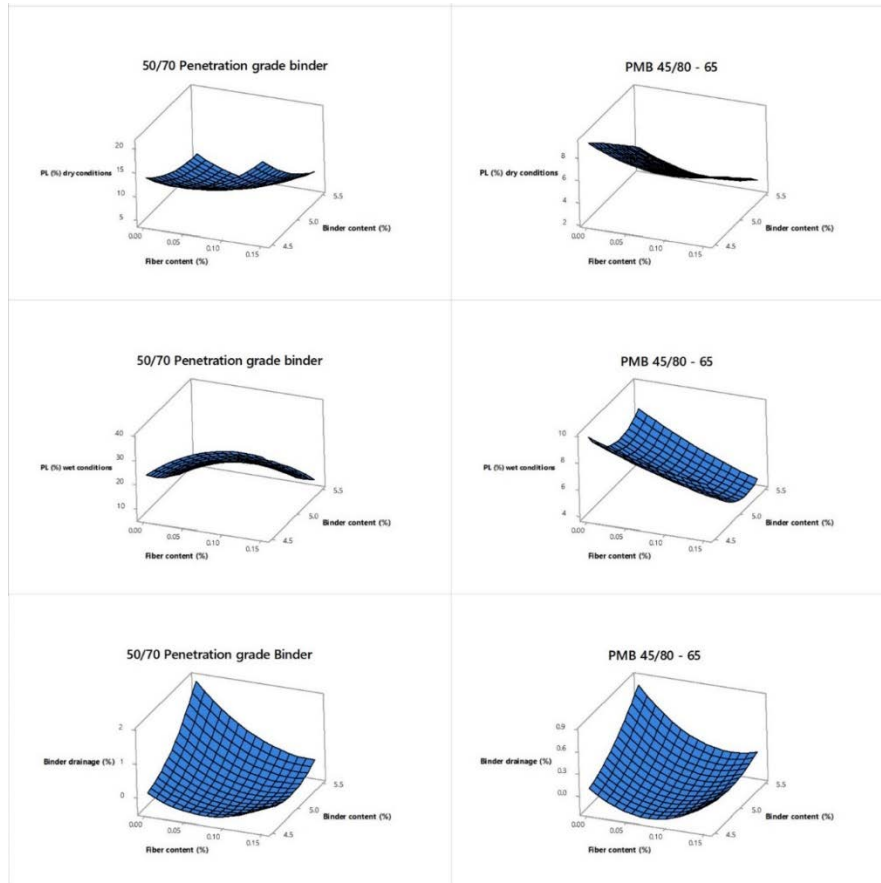369 parameter.

370

371

372
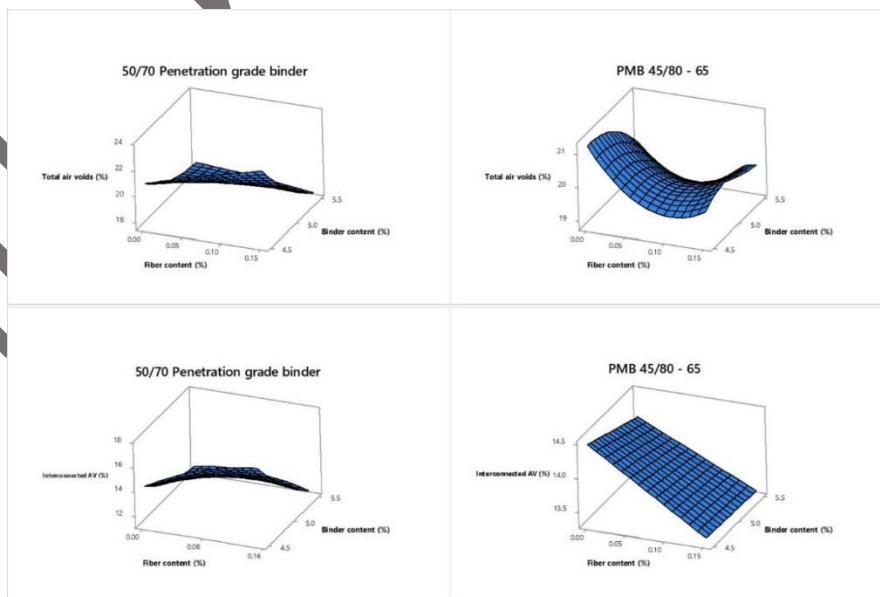
373   **Figure 9.** Interaction effect of fiber content and binder content as a function of the binder type.

374   Regarding the total and interconnected air voids, binder content (*BC*) has the highest influence, with
375   contribution factors of 82% and 80%, respectively. It means that the binder content in the mixture
376   influences notably its porosity, reducing functional performance characteristics such as permeability and
377   noise generation. On the other hand, fiber content (*FC*) seems not to have a significant effect, probably
378   because the amount of fiber used in this research is too low. Other types of fibers such as the cellulose
379   are able to reduce the amount of voids in the mixture when its content is around 0.3% by weight of
380   mixture, as suggested by other research [36]. However, the *FC* factor does have a higher influence when
381   it comes to the resulting raveling resistance responses, with contributions of 25% and 13% to the particle
382   loss in dry and wet conditions, respectively. As reported by other researchers, fibers in hot mix asphalt
383   act as a reinforcement, forming a three dimensional network inside the mixture [25,26]. In addition, fibers
384   are normally used as stabilizer agents in PA mixtures with high binder contents. The contribution of the
385   fiber content (*FC*) with regard to the binder drainage response is actually approximately 27%.

386   **Table 7.** Analysis of variance for T_{AV}, I_{AV}, PL_{DRY}, PL_{WET} and *BD*.

Variance Source	Degree of Freedom (DoF)	Adj SS	Adj MS	*F*-Value	Contribution (%)
Total air voids (%)					
Fiber content (%)	2	0.783	0.392	0.42	3.12
Binder content (%)	2	20.565	10.282	10.98	81.95
Error	4	3.747	0.937		14.93
Total	8	25.095			100.00
Interconnected air voids (%)					

Fiber content (%)	2	2.339	1.170	1.32	7.88
Binder content (%)	2	23.794	11.897	13.48	80.21
Error	4	3.531	0.883		11.90
Total	8	29.664			100.00
Particle loss—dry conditions					
Fiber content (%)	2	50.220	25.112	3.01	25.22
Binder content (%)	2	115.440	57.722	6.91	57.98
Error	4	33.420	8.354		16.79
Total	8	199.090			100.00
Particle loss—wet conditions					
Fiber content (%)	2	131.500	65.760	1.76	12.66
Binder content (%)	2	757.900	378.970	10.16	72.97
Error	4	149.100	37.290		14.36
Total	8	1038.600			100.00
Binder drainage					
Fiber content (%)	2	1.157	0.579	1.68	27.21
Binder content (%)	2	1.719	0.860	2.5	40.43
Error	4	1.375	0.344		32.34
Total	8	4.252			100.00

387 In this research, regression analyses were employed for modeling and predicting the response variables.
388 Different models were initially proposed such as linear, linear plus interactions, linear plus squares and
389 full quadratic in order to predict the best response variable. The best fitting models, those with the highest
390 R^2 values, were finally selected.
391
392 The predictive equations obtained from the analysis of the mixtures with 50/70 binder, are given below.

$$T_{AV}(\%) = 30.65 + 114 * FC(\%) - 2.194 * BC(\%) - 21.85 * FC(\%) * BC(\%) \tag{21}$$

$$I_{AV}(\%) = 25.09 + 125 * FC(\%) - 2.379 * BC(\%) - 23.52 * FC(\%) * BC(\%) \tag{22}$$

$$PL_{DRY}(\%) = 167 + 169 * FC(\%) - 57.7 * BC(\%) + 635 * FC^2(\%) + 5.23 * BC^2(\%) - 47.9 * FC(\%) * BC(\%) \tag{23}$$

$$Pl_{WET}(\%) = 352 + 649 * FC(\%) - 119 * BC(\%) - 1012 * FC^2(\%) + 10.13 * BC^2(\%) - 88.3 * FC(\%) * BC(\%) \tag{24}$$

$$BD(\%) = 27.5 + 45.6 * FC(\%) - 12.6 * BC(\%) + 80.4 * FC^2(\%) + 1.44 * BC^2(\%) - 12.63 * FC(\%) * BC(\%) \tag{25}$$

393 Similarly, the predictive equations obtained from the analysis of the mixtures with PMB 45/80-64 are as
394 follows.

$$T_{AV}(\%) = -11.5 - 72.1 * FC(\%) + 14.3 BC(\%) + 158 * FC^2(\%) - 1.57 * BC^2(\%) + 8.7 * FC(\%) * BC(\%) \tag{26}$$

$$I_{AV}(\%) = 14.4 - 28.3 * FC(\%) + 0.4 * BC(\%) + 77 * FC^2(\%) - 0.07 * BC^2(\%) + 1.9 * FC(\%) * BC(\%) \tag{27}$$

$$PL_{DRY}(\%) = 30.51 - 7.47 * FC(\%) - 4.81 * BC(\%) \tag{28}$$

15

$$PL_{WET} (\%) = 172 + 32 * FC(\%) - 64.4 * BC(\%) + 54 * FC^2(\%) + 6.28 * BC^2(\%) - 12.0 * FC(\%) * BC(\%) \tag{29}$$

$$BD (\%) = 6.7 + 12.7 * FC (\%) - 3.28 * BC(\%) + 51.6 * FC^2(\%) + 0.400 * BC^2(\%) - 4.50 * FC(\%) * BC(\%) \tag{30}$$

395 All the regression models for the mixtures using the conventional bitumen fitted very well the
396 experimental results, with R^2 values closer to 90%. Specifically, for total air voids a linear plus interaction
397 regression model was used with a R^2 value of 93.84%. A linear plus interaction regression model was used
398 also for the interconnected air voids, with a R^2 value of 96.11%. Concerning the raveling resistance, the
399 particle loss in dry and wet conditions was fitted using full quadratic regression models. In this case, R^2
400 values of 89.93% and 90.02%, respectively, were obtained. Similarly, a full quadratic regression equation
401 was used to model the binder drainage, with the R^2 being equal to 89.53%. As for the mixtures using PMB
402 45/80-65, full quadratic regression models were applied to total air voids, interconnected air voids,
403 particle loss in wet conditions and binder drainage, with R^2 values of 64.86%, 30.02%, 80.04%, and 84.00%,
404 respectively. In the case of particle loss in dry conditions, a linear regression model was applied with an
405 R^2 value of 67.07%.
406
407 Figure 10, shows the graphs where T_{AV}, I_{AV}, PL_{DRY}, PL_{WET}, and *BD* response variables were obtained
408 experimentally and those predicted by the regression model for each binder type are compared. In the
409 case of the mixtures with 50/70 penetration grade binder, predicted and experimental values are slightly
410 closer to each other as compared to the case of the mixtures with PMB 45/80-65. As an example, the
411 mean errors for the total air voids were of 1.61% and 2.01% when 50/70 penetration grade binder and
412 PMB 45/80-65 were used, respectively. For the functionality responses, results suggest that the deviation
413 between experimental data and regression models was minimal, with errors lower than 5%. However, the
414 errors in the mechanical performance responses were in the range between 10% and 20%.

415 *4.3. CRITIC Method*

416 As said before, the CRITIC methodology is employed in this research for the purpose of finding out the
417 weights of each criterion. The weights assigned to each response variable are based on the contrast
418 intensity and conflict assessment of the decision making problem [55]. According to the methodology, the
419 decision matrix is firstly normalized using Equation (13), as shown in Table 8. The standard deviation (*SD*)
420 values for all the criteria are also calculated. The correlation coefficients of the different response
421 variables were then calculated (Table 9). Finally, the weights of the different response variables were
422 determined with the help of Equations (14)–(16), as shown in Table 10.
423
424 As can be seen in Table 10, total air voids and interconnected air voids have similar weights, which is due
425 to the high correlation that exists between these two variables. On the other hand, particle loss in dry and
426 wet conditions have the highest weights, with values of 0.24 and 0.25, respectively, suggesting that
427 raveling resistance have a notable incidence in the overall performance of the PA mixture. Finally, the
428 weight assigned to binder drainage was equal to 0.17, almost equal than T_{AV} and I_{AV} weights. As is well
429 known, when weights are assigned equally, a subjective bias is involved in the decision-making process.
430 To deal with this, CRITIC approach defines the criteria weightage in an objective manner, attempting to
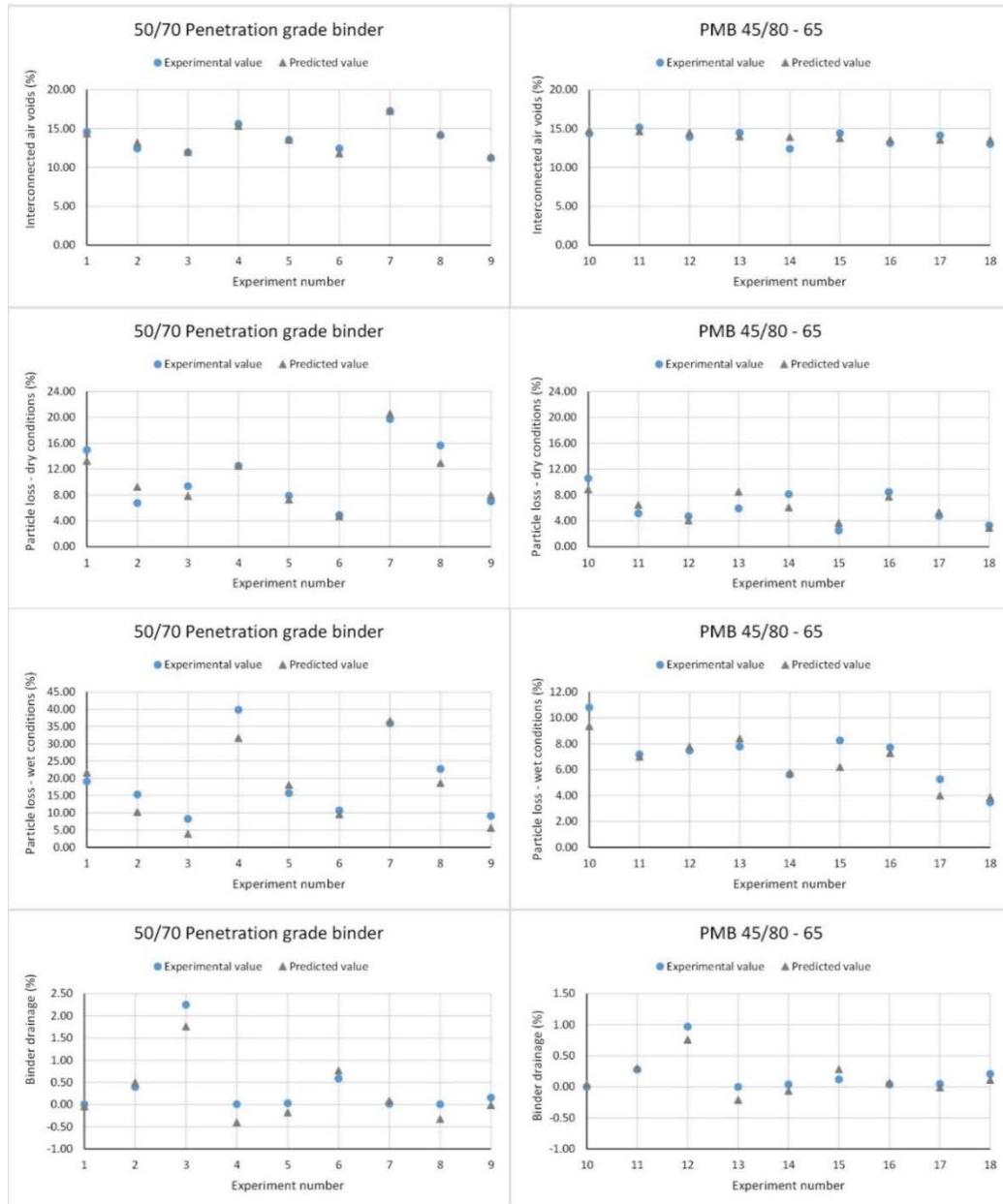431 reveal the intensity of the contrast in the decision making problem [62].
432

433

434
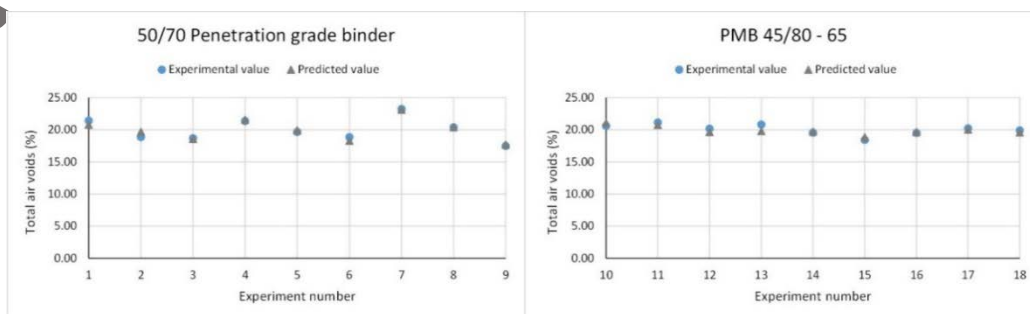
435 **Figure 10.** Experimental vs. predicted values of the different response variables.

436 **Table 8.** Normalized decision matrix for the CRITIC method.

Design	T_{AV} (%)	I_{AV} (%)	PL_{DRY} (%)	PL_{WET} (%)	BD (%)
1	0.68	0.56	0.28	0.57	1.00
2	0.24	0.20	0.75	0.67	0.82
3	0.21	0.12	0.60	0.87	0.00
4	0.68	0.72	0.42	0.00	1.00
5	0.38	0.39	0.69	0.66	0.99
6	0.24	0.20	0.86	0.80	0.74
7	1.00	1.00	0.00	0.11	0.99
8	0.50	0.48	0.24	0.47	1.00
9	0.00	0.00	0.74	0.85	0.93

17

10	0.54	0.52	0.53	0.80	1.00
11	0.63	0.65	0.85	0.90	0.88
12	0.47	0.45	0.87	0.89	0.57
13	0.58	0.54	0.80	0.88	1.00
14	0.36	0.19	0.67	0.94	0.98
15	0.16	0.53	1.00	0.87	0.95
16	0.35	0.32	0.65	0.88	0.98
17	0.48	0.49	0.87	0.95	0.98
18	0.42	0.30	0.95	1.00	0.91
SD	0.23	0.24	0.27	0.28	0.25

437

Table 9. Correlation coefficients of the different response variables.

	T_{AV} (%)	I_{AV} (%)	PL_{DRY} (%)	PL_{WET} (%)	BD (%)
T_{AV} (%)	1.00	0.89	−0.63	−0.59	0.34
I_{AV} (%)	0.89	1.00	−0.50	−0.62	0.40
PL_{DRY} (%)	−0.63	−0.50	1.00	0.79	−0.16
PL_{WET} (%)	−0.59	−0.62	0.79	1.00	−0.24
BD (%)	0.34	0.40	−0.16	−0.24	1.00

438

Table 10. Weights of the different response variables.

Criteria	C_j	W_j
T_{AV} (%)	0.93	0.18
I_{AV} (%)	0.92	0.17
PL_{DRY} (%)	1.25	0.24
PL_{WET} (%)	1.31	0.25
BD (%)	0.90	0.17

439 *4.4. TOPSIS Method*

440 In this research, the Taguchi methodology was applied for the optimization of the single responses (e.g.,
441 total air voids, interconnected air voids, etc.) in the same way that other experimental design methods
442 might have been used such as the central composite design, the response surface method or the full
443 factorial design. Moreover, in this study more than one response was evaluated and hence, it is necessary
444 to transform the multiple response variables into one single response variable. Therefore, TOPSIS
445 methodology was employed as a multi-criteria decision-making technique built into the Taguchi
446 experiment design method.
447
448 Once the weights of the different response variables were calculated by applying the CRITIC approach,
449 closeness comparative coefficient (*CCC*) for each design of experiments was determined employing
450 Equations (4)–(11). Table 11 shows the weighted normalizes decision matrix for each response variable,
451 with higher values of *CCC* indicating more optimum conditions. In this sense, the design ranked number 1
452 corresponds to the best combination of input parameters among all the set of experiments carried out.
453 The positive ideal solution (PIS) values for each response is as follows: $V_{TAV}^{+} = 0.0491$, $V_{IAV}^{+} = 0.0499$,
454 $V_{PL-dry}^{+} = 0.0149$, $V_{PL-wet}^{+} = 0.0123$ and $V_{BD}^{+} = 0.0000$. Similarly, the negative ideal solution (NIS)
455 values for each response is $V_{TAV}^{-} = 0.0370$, $V_{IAV}^{-} = 0.0324$, $V_{PL-dry}^{-} = 0.1162$, $V_{PL-wet}^{-} = 0.1410$ and
456 $V_{BD}^{-} = 0.1480$. After PIS and NIS were calculated, experiment designs were ranked based on *CCC* scores
457 (Table 11). The experimental design number 17 resulted the best design, with response values of 20.22%,

18

458 14.15%, 4.77%, 5.26%, and 0.05% for $T_{AV}, I_{AV}, PL_{DRY}, PL_{WET}$ and BD, respectively. This design involves
459 the use of polymer-modified binder with 0.15% fiber content and 5.0% binder content. On the other hand,
460 experimental design number 3 was found to be the design with the lowest CCC value and hence, the last
461 potential choice. Overall, the preference ranking of experimental designs can be given as 17 > 18 > 15 >
462 13 > 11 > 14 > 16 > 9 > 10 > 5 > 6 > 2 > 12 > 1 > 8 > 7 > 4 > 3.

463

Table 11. Weighted normalized response, CCC values and final ranking.

| Design No.	Weighted Normalized Values									
	T_{AV} (%)	I_{AV} (%)	PL_{DRY} (%)	PL_{WET} (%)	BD (%)	S_i^+	S_i^-	$S_i^+ + S_i^-$	CCC	Rank
1	0.045	0.042	0.088	0.068	0.001	0.09	0.17	0.26	0.65	14
2	0.040	0.036	0.040	0.054	0.026	0.06	0.16	0.22	0.73	12
3	0.040	0.035	0.055	0.029	0.148	0.16	0.09	0.25	0.37	18
4	0.045	0.045	0.074	0.141	0.001	0.14	0.15	0.29	0.51	17
5	0.042	0.039	0.047	0.056	0.002	0.06	0.18	0.23	0.76	10
6	0.040	0.036	0.029	0.038	0.039	0.05	0.16	0.21	0.76	11
7	0.049	0.050	0.116	0.127	0.001	0.15	0.16	0.32	0.52	16
8	0.043	0.041	0.092	0.080	0.001	0.10	0.16	0.27	0.61	15
9	0.037	0.032	0.041	0.032	0.011	0.04	0.19	0.23	0.82	8
10	0.044	0.042	0.062	0.038	0.000	0.06	0.19	0.24	0.77	9
11	0.045	0.044	0.030	0.025	0.018	0.03	0.19	0.22	0.87	5
12	0.043	0.040	0.028	0.026	0.064	0.07	0.14	0.21	0.68	13
13	0.044	0.042	0.035	0.028	0.000	0.03	0.21	0.23	0.88	4
14	0.041	0.036	0.048	0.020	0.003	0.04	0.20	0.24	0.84	6
15	0.039	0.042	0.015	0.029	0.008	0.02	0.20	0.23	0.90	3
16	0.041	0.038	0.050	0.027	0.003	0.04	0.20	0.24	0.83	7
17	0.043	0.041	0.028	0.019	0.003	0.02	0.21	0.23	0.92	1
18	0.042	0.038	0.019	0.012	0.014	0.02	0.21	0.23	0.91	2

464 CCC score values obtained via CRITIC—TOPSIS based Taguchi methodology were also used to
465 calculate the main effects plots for SNR and main effect plots for means, as shown in Figure 11.
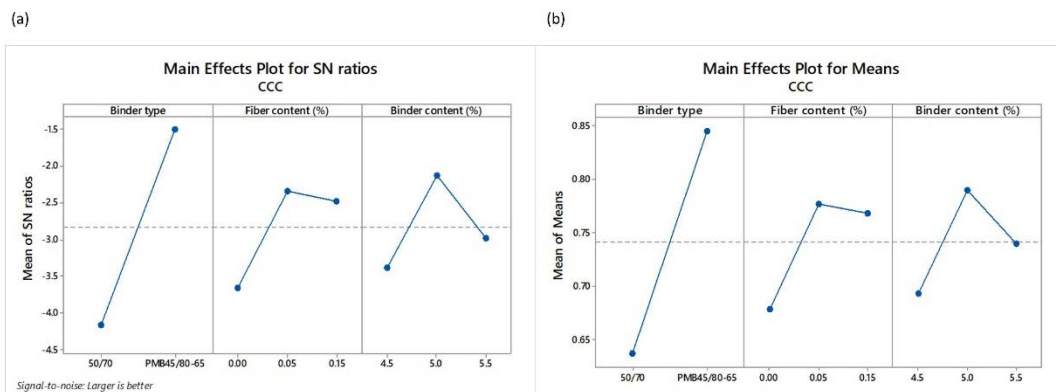
467 **Figure 11.** Main effects plots of (**a**) SNR and (**b**) means of the CCC values.

468   The type of binder seems to have the greatest impact on the SNR and means values. As can be observed
469   in the ranking, the first seven experimental designs were about mixtures using PMB. On the other hand,
470   good results were observed in terms of functionality and durability for the mixtures using 50/70
471   penetration grade binder. For example, mixtures corresponding to design number 5, with 0.05% fiber
472   content and a 5.0% binder content, exhibited particle loss values in dry and wet conditions of 7.90% and
473   15.71%, respectively. According to the scientific literature, values lower than 20% and 35% are
474   recommend in PL_{DRY} and PL_{WET} tests [2,36,37]. This mixture also shows a proper air void content of
475   approximately 20% and does not present binder drainage problems, as it obtained a drain down value
476   lower than 0.3%, the limit recommended in the literature [4].

478   When analyzing the *CCC* score values, trends indicate that low values of binder content and high values
479   of fiber content clearly affect the overall performance of mixtures using 50/70 penetration grade bitumen,
480   as can be observed in Figure 12. Likewise, all *CCC* values were below 0.80 in the case of mixtures using
481   50/70 conventional binder with the exception of design number 9, whose *CCC* value was 0.82. Moreover,
482   design number 5 scored well after design number 9 with a value of 0.76. This experimental design
483   exhibited lower values of particle loss in dry and wet conditions while maintaining admissible values of
484   total and interconnected air voids. Besides, in the case of the binder, drainage in this mixture was not
485   observed. Therefore, it could be considered as a proper mixture design. Finally, based on SNR, the TOPSIS
486   approach suggests that the optimum conditions were identified for a binder type factor equal to PMB,
487   fiber content factor of 0.05% and binder content factor of 5.0%.
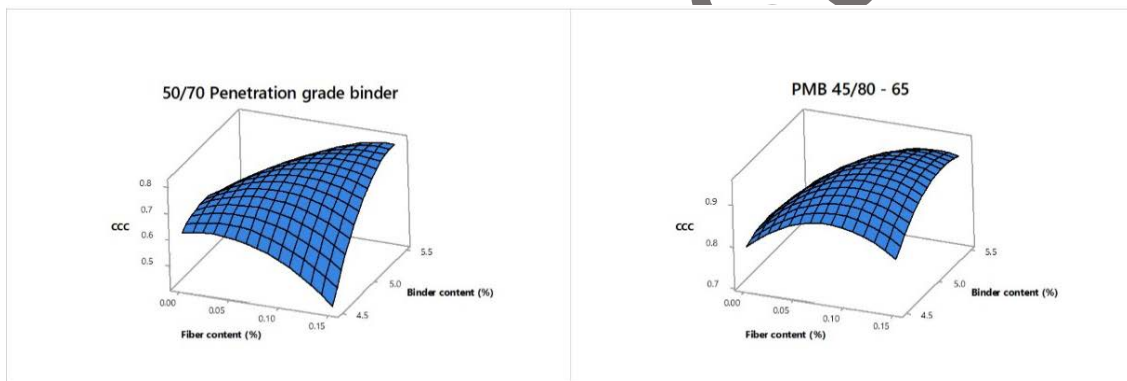
489   **Figure 12.** Interaction effect of fiber content and binder content as a function of the *CCC* score value for
490   a 50/70 penetration grade binder (left) and a PMB 45/80 - 65 (right)

491   As with the individual responses, a regression analysis was applied for the modeling of the *CCC* values and
492   the analysis of the interaction effects between input parameters and the overall *CCC* response. A linear
493   plus interaction predictive equation with a *p*-value of 0.004 significant effect was selected. The equation
494   for *CCC* are given as follows:

$$CCC = 1.128 + 0.2089 * BT - 10.84 * FC\ (\%) - 0.1049 * BC(\%) + 2.268 * FC(\%) * BC(\%). \tag{31}$$

495   The graph given in Figure 13 shows the comparison between the *CCC* response obtained through the
496   CRITIC–TOPSIS methodology and the *CCC* values from the regression model developed. The R^2 for the
497   model obtained was 66.43% and the mean error between the *CCC* values calculated via CRITIC-TOPSIS
498   and the model developed was of 11.78%. According to the analysis of variance (Table 12), the type of
499   binder has a significant effect as well was the fiber-binder interaction. In other words, the overall
500   performance of a PA mixture is linked to the proper quantities of fiber and binder, depending on the type
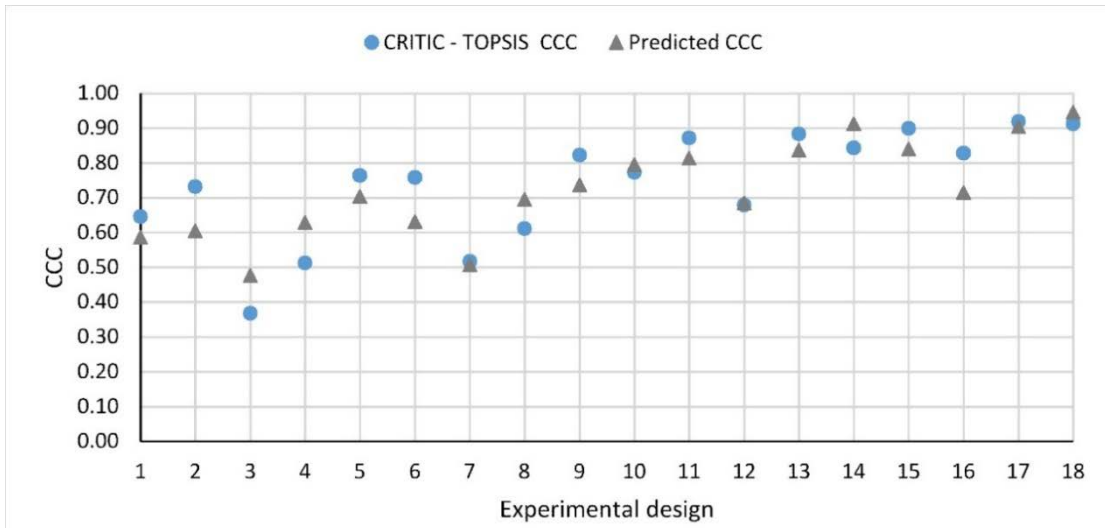501   of binder.

Figure 13. Comparison between the calculated *CCC* response and the predicted model.

Table 12. Analysis of variance of the regression model developed for *CCC*.

Source	DF	Adj SS	Adj MS	*F*-Value	*P*-Value	Significance
Model	4	0.280	0.070	6.430	0.004	Significant
Linear	3	0.226	0.075	6.930	0.005	Significant
Binder type	1	0.196	0.196	18.020	0.001	Significant
Fiber content (%)	1	0.018	0.018	1.610	0.227	
Binder content (%)	1	0.013	0.013	1.150	0.303	
2-Way Interaction	1	0.060	0.060	5.510	0.035	Significant
Fiber content (%) *Binder content (%)	1	0.060	0.060	5.510	0.035	Significant
Error	13	0.142	0.011			
Total	17	0.422				

5. Conclusions

This study presented the CRITIC-TOPSIS based on the Taguchi methodology aimed at investigating the impact of different parameters on the mechanical and functional performance of fiber reinforced porous asphalt mixtures with aramid and polyolefin fibers. A series of experiments were carried out based on the L18 Taguchi orthogonal array, and the optimal responses were identified for the total air voids, interconnected air voids, particle loss in dry conditions, particle loss in wet conditions, and binder drainage. Signal to Noise Ratio values obtained from the Taguchi design made it possible to determine the optimal levels of the control factors for the different response variables. In addition, regression models were performed with the different responses in order to evaluate the binder-fiber interaction effects as a function of the type of bitumen. Since multiple responses were obtained, a multi objective optimization was performed through the CRITIC-TOPSIS methodology. Unlike other studies that assign equal weights to the different responses, the CRITIC approach was employed in this study to find the objective criteria weights. With TOPSIS, the criteria weights were taken into account to provide a preference ranking for all the designs of experiments. Based on the results obtained, the following conclusions can be drawn:

521 • In terms of functionality, the binder content is the most influential factor on the total and
522   interconnected air voids of the mixture.
523 • Concerning the durability of the mixture, the optimum PL_{dry} response based on Signal to Noise
524   Ratio values is obtained when employing a polymer modified binder, a 0.05% fiber content, and a
525   5.5% binder content. The contribution of the fiber content is less significant when a polymer-
526   modified binder is used instead of a conventional binder.
527 • PA mixtures with a 50/70 penetration grade binder and 0.05% fiber content improve in a similar way
528   to PA mixtures with a polymer-modified binder. As for the raveling resistance, the addition of fibers
529   reduces the particle loss in dry conditions regardless of the amount of bitumen employed. However,
530   when it comes to the particle loss in wet conditions, a higher binder content seems to be necessary
531   to properly coat the fibers and hence to guarantee a higher durability under the action of water.
532 • The use of fibers in the PA mixtures not only contributed to positively mitigating the binder drainage,
533   but also to reinforcing the mixture without compromising its functionality.
534 • The best alternative according to the TOPSIS method is the design number 17. This design
535   corresponds to the use of a polymer-modified binder, 0.15% fiber content, and 5.0% binder content.
536   Although the first few positions of the order of preference refers to experiments with mixes using
537   polymer modified binder, good results can be also obtained using a conventional binder as long as
538   the proper proportions of fibers are applied.
539 • The CRITIC-TOPSIS based Taguchi can be considered a useful tool for the evaluation of the impact of
540   different admixtures on different responses, as well as for the optimization of multiple responses
541   simultaneously. It is recommended to apply this novel methodology to other composites of
542   materials.

543 **Author Contributions:** C.J.S.-A. and P.P.-M. designed the experiments. C.J.S.-A. and P.L.-G. carried out the
544 experimental plan. C.J.S.-A., P.P.-M. and P.L.-G. analyzed the data. D.C.-F. supervised the experiments. C.J.S.-A., P.P.-
545 M., P.L.-G and D.C.-F. wrote the paper. G.C.-F. is responsible for the funding acquisition. All the authors contributed
546 in the discussion of results and conclusions.

553 **References**

554 1. Nielsen, C. Durability of porous asphalt-International experience. Tech. Note 41 Copenhagen, Denmark Danish
555   Road Inst. (DRI); 2006.
556 2. Alvarez, A.E.; Martin, A.E.; Estakhri, C. A review of mix design and evaluation research for permeable friction
557   course mixtures. Constr. Build. Mater. 2011, 25, 1159–1166.
558 3. Hassan, H.F.; Al-Jabri, K.S. Effect of organic fibers on open-graded friction course mixture properties. Int. J.
559   Pavement Eng. 2005, 6, 67–75.
560 4. Mallick, R.; Kandhal, P.; Cooley Jr, L.; Watson, D. Design construction, and performance of new generation open-
561   graded friction courses; Reno Nevada, 2000;
562 5. Xu, B.; Li, M.; Liu, S.; Fang, J.; Ding, R.; Cao, D. Performance analysis of different type preventive maintenance
563   materials for porous asphalt based on high viscosity modified asphalt. Constr. Build. Mater. 2018, 191, 320–
564   329.
565 6. Chu, L.; Fwa, T.F.; Tan, K.H. Evaluation of wearing course mix designs on sound absorption improvement of
566   porous asphalt pavement. Constr. Build. Mater. 2017, 141, 402–409.
567 7. S. Shimeno, A.; T. Tanaka, O. Evaluation and further development of porous asphalt pavement with 10 years
568   experience in Japanese expressways. Proc. 11th Int Conf Asph. Pavements 2010, 1, 43–52.
569 8. Zwan, J.T. van der Developing porous asphalt for freeway in the Netherlands: Reducing noise, improving safety,
570   increasing service life. TR News 2011, 272, 22–29.

9. Liu, M.; Huang, X.; Xue, G. Effects of double layer porous asphalt pavement of urban streets on noise reduction. Int. J. Sustain. Built Environ. 2016, 5, 183–196.

10. Donavan, P.R.; Lodico, D.M. Tire/pavement noise of test track surfaces designed to replicate California highways; Washington D.C., 2009;

11. Chen, D.; Ling, C.; Wang, T.; Qian Su a, B.; Ye, A. Prediction of tire-pavement noise of porous asphalt mixture based on mixture surface texture level and distributions. Constr. Build. Mater. 2018, 173, 801–810.

12. Massahi, A.; Ali, H.; Koohifar, F.; Baqersad, M. Investigation of pavement raveling performance using smartphone. Int. J. Pavement Res. Technol. 2018, 11, 553–563.

13. Putman, B.J. Evaluation of the open graded friction courses: Construction, maintenance and performance.; 2012;

14. Senior, V.; Eliécer, J.; Maquilón, C. Resistance to degradation or cohesion loss in Cantabro test on specimens of porous asphalt friction courses . Procedia - Soc. Behav. Sci. 2014, 162, 290–299.

15. Calzada-Perez, M.A.; Perez-Jimenez, F.E. Desarrollo y normalización del ensayo de pérdida por desgaste aplicado a la caracterización, dosificación y control de mezclas bituminosas de granulometría abierta., Universidad de Cantabria, 1984.

16. Jimenez, F.E.P.; Perez, M.A.C. Analysis and evaluation of the performance of porous asphalt. The Spanish experience. ASTM Spec. Tech. Publ. First Int. Symp. Surf. Charact. State Coll. PA, USA 1988, Code 13688, 512–527.

17. Zwan, V. der; Swart, H.J.; Goeman, T.; Gruis, A.J.; Oldenburger, R.H. Porous Asphalt Wearing Courses in the Netherlands: State of the Art Review. Transp. Res. Rec. 1972, 1265.

18. Moreno-Navarro, F.; Sol-Sánchez, M.; Rubio-Gámez, M.C. The effect of polymer modified binders on the long-term performance of bituminous mixtures: The influence of temperature. Mater. Des. 2015, 78, 5–11.

19. Voskuilen, J.L.M.; Tolman, F.; Rutten, E. Do modified porous asphalt mixtures have a longer service life? 3rd Eurasphalt Eurobitume Congr. Vienna 2004.

20. Chen, J.-S.; Liao, M.-C.; Shiah, M.-S. Asphalt Modified by Styrene-Butadiene-Styrene Triblock Copolymer: Morphology and Model. J. Mater. Civ. Eng. 2002, 14, 224–229.

21. Afonso, M.L.; Dinis-Almeida, M.; Fael, C.S. Study of the porous asphalt performance with cellulosic fibres. Constr. Build. Mater. 2017, 135, 104–111.

22. Slebi-acevedo, C.J.; Lastra-gonzález, P.; Indacoechea-vega, I.; Castro-fresno, D. Laboratory assessment of porous asphalt mixtures reinforced with synthetic fibers. Constr. Build. Mater. 2020, 234.

23. Gupta, A.; Rodriguez-Hernandez, J.; Castro-Fresno, D. Incorporation of Additives and Fibers in Porous Asphalt Mixtures: A Review. Materials (Basel). 2019, 12, 3156.

24. Tanzadeh, J.; Shahrezagamasaei, R. Laboratory Assessment of Hybrid Fiber and Nano-silica on Reinforced Porous Asphalt Mixtures. Constr. Build. Mater. 2017, 144, 260–270.

25. Slebi-acevedo, C.J.; Lastra-gonzález, P.; Pascual-muñoz, P.; Castro-fresno, D. Mechanical performance of fibers in hot mix asphalt : A review. Constr. Build. Mater. 2019, 200, 756–769.

26. Abtahi, S.M.; Sheikhzadeh, M.; Hejazi, S.M. Fiber-reinforced asphalt-concrete - A review. Constr. Build. Mater. 2010, 24, 871–877.

27. Lee, S.J.; Rust, J.P.; Hamouda, H.; Kim, R.; Borden, R.H. Fatigue Cracking Resistance of Fiber-Reinforced Asphalt Concrete. Text. Res. J. 2005, 75, 123–128.

28. Yin, J.M.; Wu, W. Utilization of waste nylon wire in stone matrix asphalt mixtures. Waste Manag. 2018, 78, 948–954.

29. Fu, S.Y.; Lauke, B.; Mäder, E.; Yue, C.Y.; Hu, X. Tensile properties of short-glass-fiber- and short-carbon-fiber-reinforced polypropylene composites. Compos. Part A Appl. Sci. Manuf. 2000, 31, 1117–1125.

30. Klinsky, L.M.G.; Kaloush, K.E.; Faria, V.C.; Bardini, V.S.S. Performance characteristics of fiber modified hot mix asphalt. Constr. Build. Mater. 2018, 176, 747–752.

31. Tapkın, S.; Uşar, Ü.; Tuncan, A.; Tuncan, M. Repeated Creep Behavior of Polypropylene Fiber-Reinforced Bituminous Mixtures. J. Transp. Eng. 2009, 135, 240–249.

32. Xu, Q.; Chen, H.; Prozzi, J.A. Performance of fiber reinforced asphalt concrete under environmental temperature and water effects. Constr. Build. Mater. 2010, 24, 2003–2010.

33. Takaikaew, T.; Tepsriha, P.; Horpibulsuk, S.; Hoy, M.; Kaloush, K.E.; Arulrajah, A. Performance of Fiber-Reinforced Asphalt Concretes with Various Asphalt Binders in Thailand. J. Mater. Civ. Eng. 2018, 30, 04018193.

34. Kaloush, K.; Biligiri, K.; Zejada, W.; Rodezno, M.; Reed, J. Evaluation of Fiber-Reinforced Asphalt Mixtures Using Advanced Material Characterization Tests. J. Test. Eval. 2010, 38, 400–411.

35. Ardanuy, M.; Claramunt, J.; Toledo Filho, R.D. Cellulosic fiber reinforced cement-based composites: A review of recent research. Constr. Build. Mater. 2015, 79, 115–128.

36. Andrés-Valeri, V.C.; Rodriguez-Torres, J.; Calzada-Perez, M.A.; Rodriguez-Hernandez, J. Exploratory study of porous asphalt mixtures with additions of reclaimed tetra pak material. Constr. Build. Mater. 2018, 160, 233–239.

37. Lyons, K.R.; Putman, B.J. Laboratory evaluation of stabilizing methods for porous asphalt mixtures. Constr. Build. Mater. 2013, 49, 772–780.

38. Prasad, V.D.; Prakash, E.L.; Abishek, M.; Dev, K.U.; Kiran, C.K.S. Study on concrete containing Waste Foundry Sand , Fly Ash and Polypropylene fibre using Taguchi Method. Mater. Today Proc. 2018, 5, 23964–23973.

39. Kumar, N.R.; Ranga, C.H.; Srikant, P.; Rao, B.R. Mechanical properties of corn fiber reinforced polypropylene composites using Taguchi method. Mater. Today Proc. 2015, 2, 3084–3092.

40. Kumar Karna, S.; Sahai, R. An Overview on Taguchi Method An Overview on Taguchi Method. Int. J. Eng. Math. Sci. 2012, 1, 11–18.

41. Mehta, A.; Siddique, R.; Pratap, B.; Aggoun, S.; Łagód, G.; Barnat-hunek, D. Influence of various parameters on strength and absorption properties of fly ash based geopolymer concrete designed by Taguchi method. Constr. Build. Mater. 2017, 150, 817–824.

42. Şimşek, B.; Tansel, Y.; Şimşek, E.H. A TOPSIS-based Taguchi optimization to determine optimal mixture proportions of the high strength self-compacting concrete. Chemom. Intell. Lab. Syst. 2013, 125, 18–32.

43. Ferdous, W.; Manalo, A.; Aravinthan, T. Bond behaviour of composite sandwich panel and epoxy polymer matrix : Taguchi design of experiments and theoretical predictions. Constr. Build. Mater. 2017, 145, 76–87.

44. Teimortashlu, E.; Dehestani, M.; Jalal, M. Application of Taguchi method for compressive strength optimization of tertiary blended self-compacting mortar. Constr. Build. Mater. 2018, 190, 1182–1191.

45. Slebi-acevedo, C.J.; Silva-rojas, I.M.; Lastra-gonzález, P.; Pascual-muñoz, P.; Castro-fresno, D. Multiple-response optimization of open graded friction course reinforced with fibers through CRITIC-WASPAS based on Taguchi methodology. Constr. Build. Mater. 2020, 233, 117274.

46. Jato-Espino, D.; Castillo-Lopez, E.; Rodriguez-Hernandez, J.; Canteras-Jordana, J.C. A review of application of multi-criteria decision making methods in construction. Autom. Constr. 2014, 45, 151–162.

47. Zhang, X.; Zhang, Q.; Sun, T.; Zou, Y.; Chen, H. Evaluation of urban public transport priority performance based on the improved TOPSIS method: A case study of Wuhan. Sustain. Cities Soc. 2018, 43, 357–365.

48. Jato-espino, D.; László, I.I.; Daniel, G. Decision support model for the selection of asphalt wearing courses in highly trafficked roads. Soft Comput. 2018, 22, 7407–7421.

49. Egle, Š.; Jurgita, A. Solving the problems of daylighting and tradition continuity in a reconstructed vernacular building. J. Civ. Eng. Manag. 2013, 19, 873–882.

50. Salih, M.M.; Zaidan, B.B.; Zaidan, A.A.; Ahmed, M.A. Survey on fuzzy TOPSIS state-of-the-art between 2007 and 2017. Comput. Oper. Res. 2019, 104, 207–227.

51. Ertugrul, I.; Karakasoglu, N. Fuzzy TOPSIS method for academic member selection in engineering faculty. Innov. E-learning, Instr. Technol. Assessment, Eng. Educ. 2007, 151–156.

52. Diakoulaki, D.; Mavrotas, G.; Papayannakis, L. D E T E R M I N I N G OBJECTIVE WEIGHTS IN M U L T I P L E CRITERIA PROBLEMS : THE CRITIC M E T H O D. Comput. Oper. Res. 1995, 22, 763–770.

53. Rostamzadeh, R.; Ghorabaee, M.K.; Govindan, K.; Esmaeili, A.; Nobar, H.B.K. Evaluation of sustainable supply chain risk management using an integrated fuzzy TOPSIS- CRITIC approach. J. Clean. Prod. 2018, 175, 651–669.

54. Kumari, M.; Kulkarni, M.S. Single-measure and multi-measure approach of predictive manufacturing control: A comparative study. Comput. Ind. Eng. 2019, 127, 182–195.

55. Kumari, M.; Kulkarni, M.S. A unified index for proactive shop floor control. Int. J. Adv. Manuf. Technol. 2019, 100, 2435–2454.

56. Gopal, P.M.; Soorya Prakash, K. Minimization of cutting force, temperature and surface roughness through GRA, TOPSIS and Taguchi techniques in end milling of Mg hybrid MMC. Meas. J. Int. Meas. Confed. 2018, 116, 178–192.

57. PG-3 Pliego de prescripciones técnicas generales para obras de carreteras y puentes. Art. 542. Mezclas bituminosas tipo hormigón bituminoso. 2015, 514 p.

675   58.   Alvarez, A.E.a, B.; Martin, A.E..; Estakhri, C..; Izzo, R.. Determination of volumetric properties for permeable
676   friction course mixtures. J. Test. Eval. 2009, 39, 1–10.
677   59.   Wang, X.; Gu, X.; Jiang, J.; Deng, H. Experimental analysis of skeleton strength of porous asphalt mixtures.
678   Constr. Build. Mater. 2018, 171, 13–21.
679   60.   Nikolaides, A. Highway engineering. Pavements, materials and control quality.; 1th editio.; CRC press – Taylor
680   and Francis group, 2017; ISBN 9781138893764.
681   61.   Mahmud, M.Z.H.; Hassan, N.A.; Hainin, M.R.; Ismail, C.R. Microstructural investigation on air void properties of
682   porous asphalt using virtual cut section. Constr. Build. Mater. 2017, 155, 485–494.
683   62.   Adalı, E.A.; Işık, A.T. Critic and Maut Methods for the Contract Manufacturer Selection Problem. Eur. J.
684   Multidiscip. Stud. 2017, 5, 93.
685